

Optimum active power tracking based control of brushless doubly-fed reluctance generator tied to renewable microgrid

Adikanda Parida, Manish Paul

Department of Electrical Engineering, North Eastern Regional Institute of Science and Technology, Nirjuli, India

Article Info

Article history:

Received Apr 18, 2023

Revised Jul 2, 2023

Accepted Jul 20, 2023

Keywords:

Brushless DFRG

Energy efficiency

Parameter sensitivity

Renewable energy

Wind energy generation system

ABSTRACT

Among all the existing wind energy generators (WEG), a brushless doubly-fed reluctance generator (BDFRG) is the better option in terms of maintenance cost and constructional simplicity. For more adaptability, the efficiency of the BDFRG can be improved through proper control mechanisms. Therefore, this paper presents an optimum active power tracking-based control technique for BDFRG for minimum losses. Copper loss of the machine is considered to be the objective function for the proposed optimization technique. However, one issue found to be the major in all the existing controllers is the accuracy of sensor less control of the BDFRG. Therefore, this paper proposes an accurate model reference adaptive system (MRAS) based sensor less mechanism for computation of BDFRG secondary winding flux position. The no sensitivity of the proposed technique to the machine parameter variation and hence the accuracy, catch-on-fly, and non-inclusion of integrator and differentiators and hence less burden on the processor makes the proposed scheme robust. The control scheme is practically implemented with a 2.5 kW BDFRG using MATLAB/Simulink platform.

This is an open access article under the [CC BY-SA](https://creativecommons.org/licenses/by-sa/4.0/) license.



Corresponding Author:

Adikanda Parida

Department of Electrical Engineering, North Eastern Regional Institute of Science and Technology

Nirjuli, India

Email: ap@nerist.ac.in

NOMENCLATURE

$\omega_r, \omega_p, \omega_s$: Angular speed of the BDFRG rotor, primary winding flux, secondary winding flux in rad./sec
$V_{pd}, V_{pq}, i_{pd}, i_{pq}$: dq-axis primary winding voltages, currents of BDFRG
$V_{sd}, V_{sq}, i_{sd}, i_{sq}$: dq-axis secondary winding voltages, currents of BDFRG
L_p, L_s	: Primary, secondary winding self-inductances
L_m	: Mutual inductance between stator and rotor
P_p, P_s	: Primary, secondary winding active power
λ_p, λ_s	: Primary, secondary flux
Superscript	: e, s, p; synchronous, secondary, and primary reference frames

1. INTRODUCTION

A brushless doubly-fed reluctance machine is an updated form of induction machine involved in power generation from wind. Although there is a similarity between the doubly-fed induction generator (DFIG) and brushless doubly-fed reluctance generator (BDFRG), in comparison to DFIG, BDFRG is gaining popularity because of its simple construction, robustness in control, and improved efficiency [1]–[3]. The

secondary winding is connected to the grid through a bi-directional converter, which ensures power flow between the primary and secondary winding [4]. It has a high saliency reluctance rotor and the numbers of salient poles are equal to the total number of pole pairs in the stator [5]. Due to the absence of brushes and slip rings, the performance and efficiency are better and make this a good contender for wind power generation applications, which substitute the DFIG. There are various existing control techniques available for the active and reactive powers of the BDFRG. A flux-oriented vector control mechanism for BDFRG is presented in [6], [7]. Different scalar control strategies are presented in [8], [9]. Also, different vector control techniques are presented in [10]–[15]. However, none of the authors have mentioned the optimum active power tracking of the controller for the minimization of copper losses both in the primary and control winding of the BDFRG. In this paper, an optimum active power tracking-based control mechanism has been presented for minimum copper losses of BDFRG. Initially, the reference active power is computed for minimum copper losses of the machine with the help of measured and known variables. Then the instantaneously computed active power is allowed to track its reference counterpart. As there is much similarity in the rotating principle between the DFIG and BDFRG, therefore in this paper, an MRAS-based rotor position and speed estimation technique is implemented for sensor less control as presented in [16]–[20]. The presented MRAS technique used for rotor position and speed computation of BDFRG considers the active power of the machine as the adjustable variable and is not sensitive to the machine parameter variations unlike the mechanism presented in [21]–[24]. The overall proposed scheme is shown in Figure 1. The highlights of the proposed control technique can be summarized as follows:

- i) Unlike the earlier BDFRG control techniques, the proposed control technique improves efficiency.
- ii) The secondary winding flux position computation algorithm developed is non-sensitive to the machine parameter variations. Thus accurate.
- iii) The algorithm developed for the secondary winding flux position computation does not uses differentiators and integrators. Thus, putting less burden on the processor.
- iv) The algorithm developed for the secondary winding flux position computation exhibits the property of catch-on-fly. Thus, robust for wide wind speed variation applications.

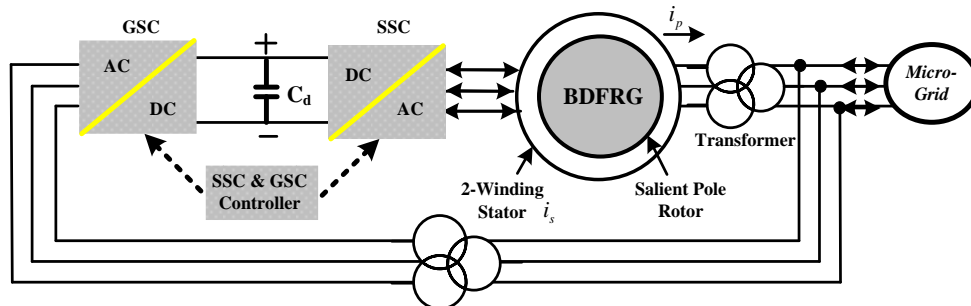


Figure 1. Overall proposed wind energy-based generation scheme

2. PROPOSED CONTROL MECHANISM

2.1. Modeling of BDFRG

Unlike the DFIG, the brushless doubly-fed reluctance generator consists of two sinusoidal distributed winding in the stator. While the primary winding works at grid frequency, the control or secondary winding operates at a different frequency i.e. at the rotor frequency of the BDFRG. The d-q axis primary winding voltage expression is presented in (1) and that of secondary or winding in (2) in the synchronous reference frame. The vector positions of different variables are shown in Figure 2.

$$V_{pd}^e = R_p i_{pd}^e + \frac{d\lambda_{pd}^e}{dt} - \omega_p \lambda_{pq}^e; V_{pq}^e = R_p i_{pq}^e + \frac{d\lambda_{pq}^e}{dt} + \omega_p \lambda_{pd}^e \tag{1}$$

$$V_{sd}^e = R_s i_{sd}^e + \frac{d\lambda_{sd}^e}{dt} - (\omega_p - \omega_s) \lambda_{sq}^e; V_{sq}^e = R_s i_{sq}^e + \frac{d\lambda_{sq}^e}{dt} + (\omega_p - \omega_s) \lambda_{sd}^e \tag{2}$$

Similarly, d-q axis primary winding currents as (3).

$$i_{pd}^e = \frac{(\lambda_{pd}^e - L_m i_{sd}^e)}{L_p}; i_{pq}^e = \frac{(\lambda_{pq}^e + L_m i_{sq}^e)}{L_p} \tag{3}$$

Similarly, the secondary winding current can be as (4).

$$i_{sd}^e = \frac{(\lambda_{sd}^e - L_m i_{pd}^e)}{L_s}; \quad i_{sq}^e = \frac{(\lambda_{sq}^e + L_m i_{pq}^e)}{L_s} \quad (4)$$

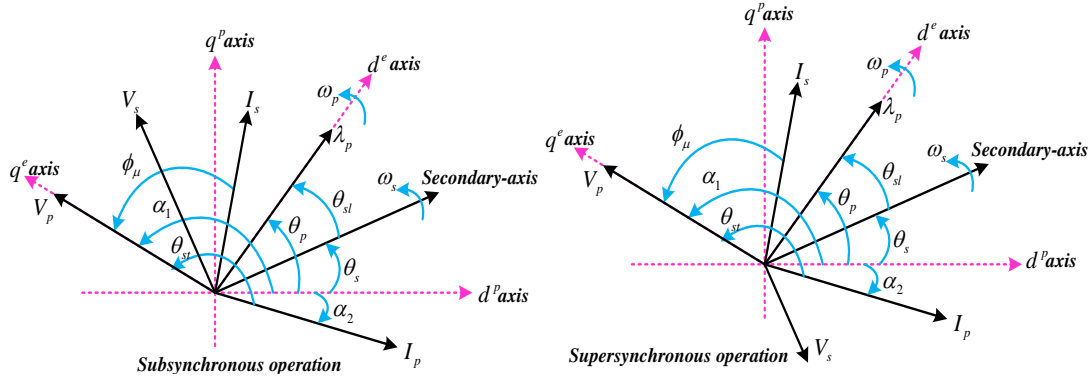


Figure 2. Primary and secondary winding variables phasor

2.2. Modeling of the controller

The rating of the BDFRG is known for its active power generated at the primary winding. The stator's active power will remain always at 1p. u. During super synchronous operation, when the active power exceeds 1p. u, the excess active power of the machine will be supplied to the grid through the secondary winding. Similarly, during subsynchronous operation of the BDFRG, to maintain primary winding active power at 1p. u, the shortage of power will be recirculated through the secondary winding and the marginal active power loss due to power circulation is generally compensated by the microgrid. This power exchange process through the secondary winding will be accomplished through the secondary side converter (SSC) control mechanism with the help of the secondary grid side converter (GSC).

The primary active power of the BDFRG can be as (5).

$$P_p = \left(\frac{3}{2}\right) (V_{pd}^e i_{pd}^e + V_{pq}^e i_{pq}^e) \quad (5)$$

As the resistive drop in the primary winding is insignificant to the terminal voltage, at steady-state, (1) will be reduced to (6).

$$V_{pd}^e = -\omega_p \lambda_{pq}^e; \quad V_{pq}^e = \omega_p \lambda_{pd}^e \quad (6)$$

Substituting, (6) in (5), the primary winding active power can be expressed in terms of primary flux as (7).

$$P_p = \left(\frac{3\omega_p}{2}\right) (\lambda_{pd}^e i_{pd}^e - \lambda_{pq}^e i_{pq}^e) \quad (7)$$

Aligning the primary flux along the d-axis, (7) reduced to (8).

$$P_p = \left(\frac{3\omega_p}{2}\right) \lambda_{pd}^e i_{pd}^e \quad (8)$$

The BDFRG copper loss considering both primary and secondary winding can be written as (9).

$$P_{ps}^{cu} = R_p [(i_{pd}^e)^2 + (i_{pq}^e)^2] + R_s [(i_{sd}^e)^2 + (i_{sq}^e)^2] \quad (9)$$

Substituting for i_{sd}^e and i_{sq}^e from (4) in (9) with $\lambda_{pq}^e = 0$.

$$P_{ps}^{cu} = R_p [(i_{pd}^e)^2 + (i_{pq}^e)^2] + \left(\frac{R_s L_p^2}{L_m^2}\right) (i_{pd}^e)^2 + \left(\frac{R_s}{L_m^2}\right) [(\lambda_{pd}^e)^2 + L_p^2 (i_{pd}^e)^2 - 2L_p i_{pd}^e \lambda_{pd}^e] \quad (10)$$

For minimum copper loss at optimum flux as (11).

$$\frac{\partial P_{ps}^{cu}}{\partial \lambda_{pd}^e} = 0 \Rightarrow \left(\frac{R_s}{L_m^2}\right) [2\lambda_{pd}^e - 2L_p i_{pd}^e] = 0 \Rightarrow \lambda_{pd}^e = L_p i_{pd}^e \tag{11}$$

Also, $\frac{\partial^2 P_{ps}^{cu}}{\partial (\lambda_{pd}^e)^2} = \frac{R_s}{L_m^2} > 0$. Which is the condition for the minima. Substituting, (11) in (8), the optimum value of the primary winding active power can be computed for known values of primary frequency and primary winding self-inductance as (12).

$$P_p^{Opt} = (1.5\omega_p)L_p i_{pd}^e i_{pq}^e \tag{12}$$

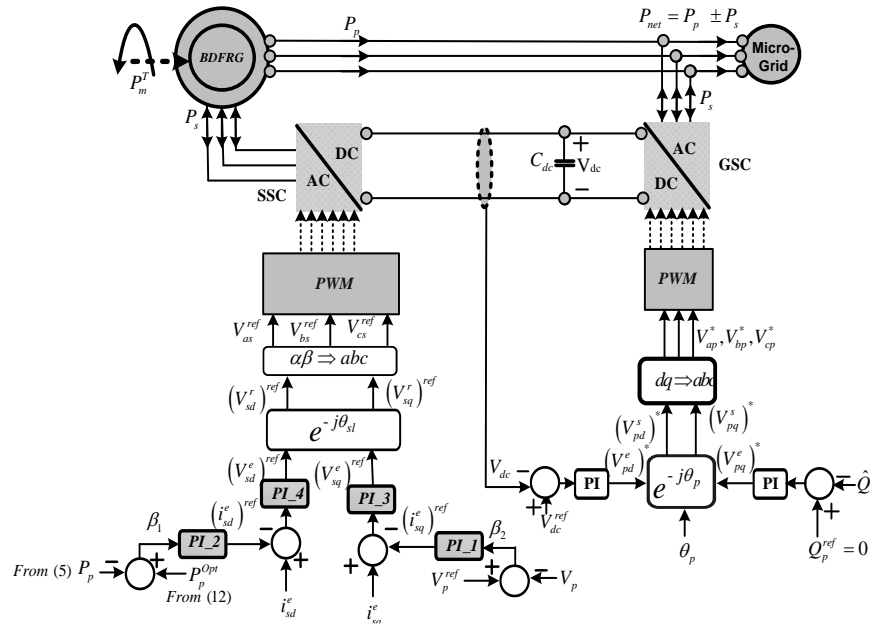


Figure 3. Details of the proposed control mechanism

The proposed scheme is shown in Figure 3, where the SSC is controlled through two control loops. In loop-1, the instantaneous primary active power as in (5) tracks its optimum counterpart as computed in (12). Therefore, the total copper losses in the BDFRG minimize at all operating points through loop-1 control. Similarly, the primary winding terminal rated voltage level is ensured through the loop-2 control as shown in Figure 3. Where the instantaneous measured voltage is tracking its reference counterpart. In the proposed control scheme, the secondary flux position has been measured accurately through the proposed sensorless technique as presented in section 3. It can be observed from Figure 3 that $\theta_{slip} = \theta_p - \theta_s$ is a piece of vital information that majorly decides the accuracy of the control. Therefore, θ_s must be computed accurately. The pulse width modulation (PWM) technique is used to control the bidirectional power exchange between the DC-link and the secondary winding of the BDFRG as shown in Figure 3. Similarly, the GSC is controlled through two control loops. While loop-1 ensures the constant DC-link voltage, loop-2 ensures the power factor close to 1 of the generation system.

3. COMPUTATION OF STATIONARY FLUX POSITION

It is already said, the accuracy of all the existing controllers including the proposed one is highly dependent on the secondary flux position information of the BDFRG. In this paper, a model reference adaptive system (MRAS) based secondary flux position computation scheme has been proposed and the same has been implemented using the proposed controller. In this MRAS model, primary winding active power is considered to be the adjustable variable. Considering (5), and substituting (3) in (5) for $\lambda_{pq}^e = 0, V_{pd}^e \approx 0$.

$$P_p^* = \left(\frac{3}{2}\right) V_{pq}^e i_{pq}^e; \hat{P}_p = \left[\frac{3}{2(1+\sigma_s)}\right] V_{pq}^e i_{sq}^e \tag{13}$$

Where, $\sigma_s = \frac{L_{lp}}{L_m} \approx 0, \sigma_s$ called the primary winding leakage factor. For the proposed MRAS, the reference primary adjustable active power \hat{P}_p is compared with its reference counterpart P_p^* . The error signal ε generated from the comparison is processed through a PI controller for the computation of secondary flux rotating speed ω_p . The same has been integrated to compute the position of the secondary flux θ_p as shown in Figure 4. The proposed MRAS model has been tested using the MATLAB-Simulink software platform and the performance is shown in Figure 5.

Regarding parameter sensitivity, the factor which can influence the adjustable variable in (13) is the factor $(1 + \sigma_s) = K$. Assuming, variation in L_m by ΔL_m which changes the influencing factor K to $K + \Delta K$. Therefore, $K + \Delta K = 1 + \frac{1}{L_m + \Delta L_m}$ and $\Delta K = L_{ls} \left[\frac{-\Delta L_m}{L_m(L_m + \Delta L_m)} \right]$. As $\Delta L_m \ll L_m$ ΔK reduces to zero. Therefore, the proposed MRAS model remains almost unbiased from BDFRG magnetizing inductance variations. To validate the above statement, the L_m value has been increased by 50% and the performance of the scheme is tested. It has been observed from Figure 5(a) that the proposed MRAS model computes the position of the secondary winding flux with almost zero computational error. Similarly, from Figure 5(b), it can be observed that the system exhibits excellent performance for a reduced magnetizing inductance by 50%.

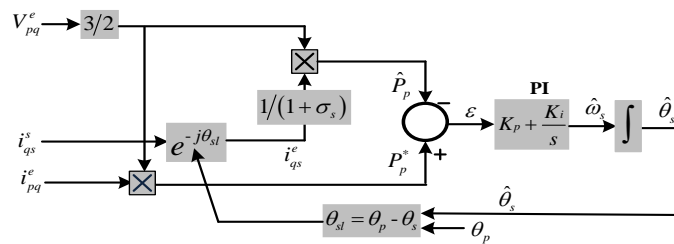


Figure 4. Implemented MRAS model

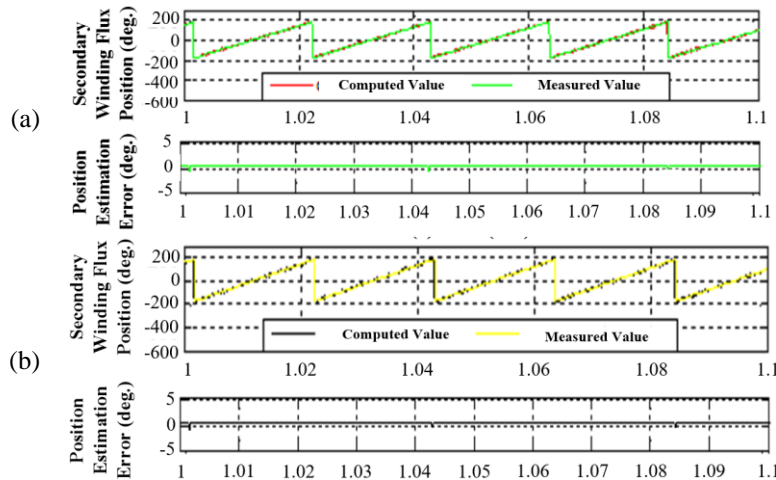


Figure 5. Parameter sensitivity of the proposed MRAS, (a) L_m variation by +50% and (b) L_m variation by -50%

4. THE TEST RESULTS

Two 500 KVA transformers in parallel feeding power to the power pool along with an 800 KVA diesel generator with variable domestic and institutional loading is considered to be the microgrid for this experiment. A prototype experimental setup consists of a 2.5 kW BDFRG, a 5 kW DC separately excited motor used as the wind turbine emulator, a 1 kW back-to-back SSC and GSC connected between the secondary and primary winding of the BDFRG with necessary control arrangement, a dSPACE (CP1104) module along with an appropriate PC interface, 3 numbers DSOs (214 C, 1000 MHz), a power analyzer (Fluke 435) and a 2 kW local R-L load augmented with BDFRG terminals as shown in Figure 6. Also, the proposed scheme is simulated using MATLAB/Simulink.

Out of the many simulation results, some of the relevant results are presented here to validate the effectiveness of the proposed controller. The output of the proposed MRAS scheme is shown in Figure 7 where the computed speed of the secondary flux is shown in Figure 7(a) during the speed transition. To test the catch-on-fly behavior of the proposed MRAS scheme, the rotor speed is varied from sub synchronous speed to super synchronous speed through synchronous speed. From Figure 7(b), it can be observed that the proposed model precisely computes the secondary flux speed with insignificant estimation error as shown in Figure 7(c). The corresponding computed secondary flux position can be observed from Figure 7(d) near synchronous speed with almost zero computational error as shown in Figure 7(e).

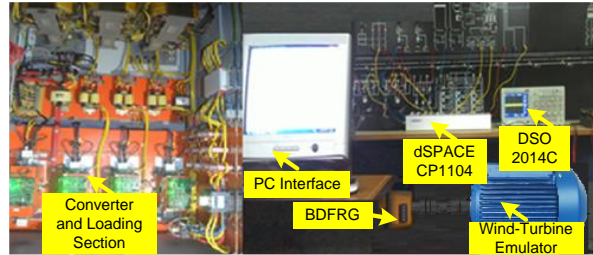


Figure 6. Testing setup

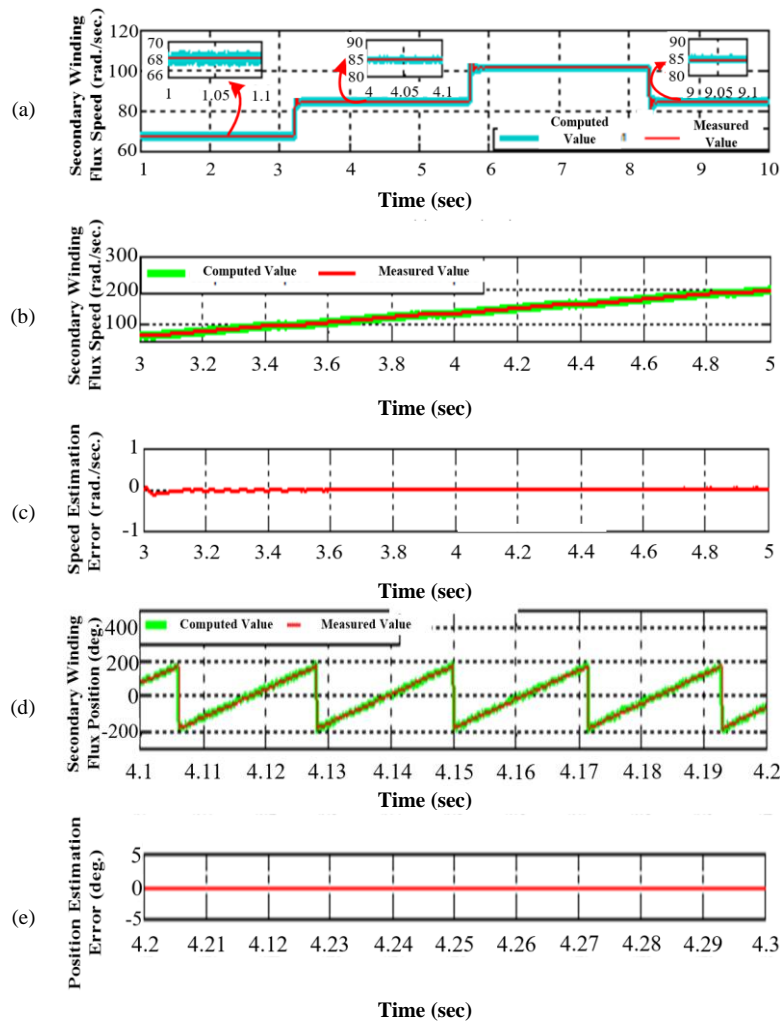


Figure 7. Computation of Secondary flux speed/position; (a) secondary winding flux speed computation under transient condition, (b) computation of secondary winding flux speed during speed transition from sub synchronous to super synchronous region, (c) flux speed computation error, (d) computation of secondary winding flux position during speed transition as in (b), and (e) flux position computation error

Out of the total feasible results captured to validate the performance of the proposed controller, four relevant results are presented as shown in Figure 8. As it is already said, irrespective of the rotor speed within the operating range, the primary active power remains at 1 p.u. The same can be observed in Figure 8(a). Where the active power remains constant at 2.2 kW even though the turbine speed varies randomly within the operating range. As the turbine output power varies, the quantity and direction of active power at the secondary winding of the BDFRG through the DC-link will also vary proportionately. Therefore, the net power supposed to be fed to the microgrid will vary. The same can be observed in Figure 8(b) and Figure 8(c). Since the proposed scheme has been designed to operate at unit power factor (UPF), it has been observed that the reactive power delivery for the proposed scheme is almost negligible as shown in Figure 8(d). From the input and output power information, with known values of the constant losses, the copper loss for the BDFRG has been computed with and without using the proposed controller. The same has been provided in Table 1. It has been observed that the proposed controller effectively improves the efficiency of the machine as the average copper loss is reduced almost by 0.68%. For wind energy-dominated microgrids, the energy saved through improved efficiency not only improve the economic sustainability of the generation companies (GENCOs) but also considerably reduces the maintenance cost of the system. Moreover, for the BDFRGs of higher ratings, the improved efficiency operation will increase the life expectancy of the generator.

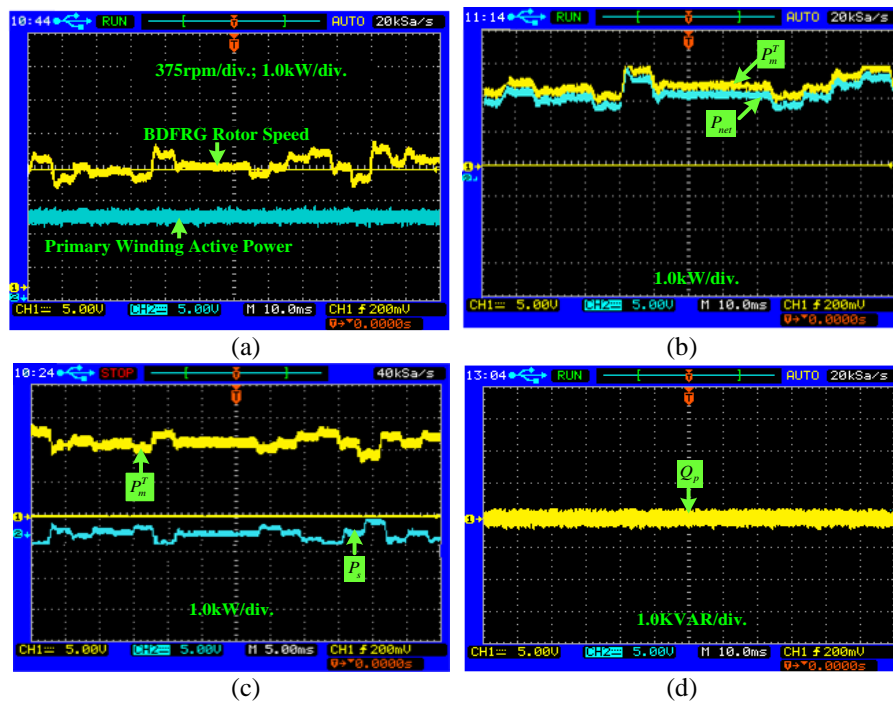


Figure 8. Performance of the controller; (a) primary active power in response to the variation of BDFRG rotor speed, (b) response of net active power generated from the BDFRG as the turbine output varies randomly, (c) secondary winding active power variation of BDFRG Primary winding as the turbine output varies randomly, and (d) reactive power measured at the primary winding terminals of BDFRG

Table 1. Comparison of Cu-loss with the proposed scheme

Slip	P_s (kW)	V_s (V)	Cu-Loss without optimum control (Watt) [7], [25]	Cu-Loss with the proposed controller (Watt)
0.30	0.750	110	101.5	88.10
0.25	0.625	110	94.10	82.15
0.20	0.500	110	88.71	79.35
0.15	0.375	110	84.21	78.20
0.10	0.250	110	81.00	77.25
0.05	0.125	110	79.20	76.50
0.00	0.003	110	78.50	76.25
-0.05	-0.125	110	79.00	77.50
-0.10	-0.250	110	81.00	76.00
-0.15	-0.375	110	84.00	77.50
-0.20	-0.500	110	88.00	78.00
-0.25	-0.625	110	94.50	79.10
-0.30	-0.750	110	102.2	79.8

5. CONCLUSION

The optimum active power tracking-based BDFRG control algorithm has been developed and the same has been successfully implemented. The mathematically developed SSC controller has been simulated and the results observed indicate the effectiveness of the scheme. The tested scheme has been implemented with the mentioned hardware with a virtual microgrid system. The proposed scheme exhibits significant improvement in the efficiency of the BDFRG over the entire operating range. It has been observed that the proposed scheme reduces average copper loss almost by 0.68%. Though the scheme has been implemented with a prototype system, it can be extended to higher-scale systems for better performance. Even though it is beyond the scope of this paper, for the efficiency improvement of BDFRG, only copper loss has been considered as the objective function, however, total loss of the BDFRG can be considered as the objective function to improve the efficiency further. Therefore, the proposed scheme will increase the active power generation capability, reduce maintenance costs, and increase the generator's life expectancy.




REFERENCES

- [1] R. E. Betz and M. G. Jovanovic, "Theoretical analysis of control properties for the brushless doubly fed reluctance machine," *IEEE Transactions on Energy Conversion*, vol. 17, no. 3, pp. 332–339, Sep. 2002, doi: 10.1109/TEC.2002.801997.
- [2] S. Khaliq, M. Modarres, T. A. Lipo, and B. Il Kwon, "Design of Novel Axial-Flux Dual Stator Doubly Fed Reluctance Machine," *IEEE Transactions on Magnetics*, vol. 51, no. 11, pp. 1–4, 2015, doi: 10.1109/TMAG.2015.2444382.
- [3] Fengxiang Wang, Fengge Zhang, and Longya Xu, "Parameter and performance comparison of doubly fed brushless machine with cage and reluctance rotors," *IEEE Transactions on Industry Applications*, vol. 38, no. 5, pp. 1237–1243, Sep. 2002, doi: 10.1109/TIA.2002.802917.
- [4] L. Xu, L. Zhen, and E. H. Kim, "Field-orientation control of a doubly excited brushless reluctance machine," *Conference Record of the 1996 IEEE Industry Applications Conference Thirty-First IAS Annual Meeting*, San Diego, CA, USA, 1996, pp. 319–325 vol.1, doi: 10.1109/IAS.1996.557039.
- [5] A. M. Knight, R. E. Betz, and D. Dorrell, "Design and analysis of brushless doubly fed reluctance machines," *IEEE Energy Conversion Congress and Exposition: Energy Conversion Innovation for a Clean Energy Future, ECCE 2011, Proceedings*, pp. 3128–3135, 2011, doi: 10.1109/ECCE.2011.6064190.
- [6] S. Ademi and M. Jovanovic, "Control of doubly-fed reluctance generators for wind power applications," *Renewable Energy*, vol. 85, pp. 171–180, 2016, doi: 10.1016/j.renene.2015.06.040.
- [7] M. R. A. Kashkooli and M. G. Jovanović, "Sensorless adaptive control of brushless doubly-fed reluctance generators for wind power applications," *Renewable Energy*, vol. 177, pp. 932–941, 2021, doi: 10.1016/j.renene.2021.05.154.
- [8] M. Jovanovic, "Sensored and sensorless speed control methods for brushless doubly fed reluctance motors," *IET Electric Power Applications*, vol. 3, no. 6, pp. 503–513, 2009, doi: 10.1049/iet-epa.2008.0227.
- [9] M. G. Jovanovic, R. E. Betz, and J. Yu, "The use of doubly fed reluctance machines for large pumps and wind turbines," *IEEE Transactions on Industry Applications*, vol. 38, no. 6, pp. 1508–1516, Nov.-Dec. 2002, doi: 10.1109/TIA.2002.804749.
- [10] A. B. Attaya, S. Ademi, M. Javanovic, and O. Anaya-Lara, "Frequency support using doubly fed induction and reluctance wind turbine generators," *Internal Journal of Electrical Power and Energy Systems*, vol. 101, pp. 403–414, 2018, doi: 10.1016/j.ijepes.2018.04.007.
- [11] M. G. Jovanović, J. Yu, and E. Levi, "Encoderless direct torque controller for limited speed range applications of brushless doubly fed reluctance motors," *IEEE Transactions on Industry Applications*, vol. 42, no. 3, pp. 712–722, 2006, doi: 10.1109/TIA.2006.872955.
- [12] S. Liang, S. Jin, and L. Shi, "Research on Control Strategy of Grid-connected Brushless Doubly-fed Wind Power System Based on Virtual Synchronous Generator Control," *CES Transactions on Electrical Machines and Systems*, vol. 6, no. 4, pp. 404–412, 2022, doi: 10.30941/CESTEMS.2022.00052.
- [13] M. Kumar, S. Das, and K. Kiran, "Sensorless Speed Estimation of Brushless Doubly-Fed Reluctance Generator Using Active Power Based MRAS," *IEEE Transactions on Power Electronics*, vol. 34, no. 8, pp. 7878–7886, 2019, doi: 10.1109/TPEL.2018.2882473.
- [14] M. Moazen, R. Kazemzadeh, M.-R. Azizian, "Mathematical proof of BDFRG model under unbalanced grid voltage condition," *Sustainable Energy, Grids and Networks*, vol. 21, 2020, doi: 10.1016/j.segan.2020.100327.
- [15] M. R. Agha Kashkooli and M. G. Jovanovic, "A MRAS Observer Based Sensorless Control of Doubly-Fed Reluctance Wind Turbine Generators," *IECON Proceedings (Industrial Electronics Conference)*, vol. 2020-October, pp. 1734–1739, 2020, doi: 10.1109/IECON43393.2020.9255202.
- [16] A. Parida, S. Choudhury, and D. Chatterjee, "Microgrid Based Hybrid Energy Co-Operative for Grid-Isolated Remote Rural Village Power Supply for East Coast Zone of India," *IEEE Transactions on Sustainable Energy*, vol. 9, no. 3, pp. 1375–1383, 2018, doi: 10.1109/TSTE.2017.2782007.
- [17] A. Parida and D. Chatterjee, "Cogeneration topology for wind energy conversion system using doubly-fed induction generator," *IET Power Electronics*, vol. 9, no. 7, pp. 1406–1415, 2016, doi: 10.1049/iet-pel.2015.0581.
- [18] A. Parida and D. Chatterjee, "Stand-alone AC-DC microgrid-based wind-solar hybrid generation scheme with autonomous energy exchange topologies suitable for remote rural area power supply," *International Transactions on Electrical Energy Systems*, vol. 28, no. 4, 2018, doi: 10.1002/etep.2520.
- [19] A. Parida and D. Chatterjee, "Integrated DFIG-SCIG-based wind energy conversion system equipped with improved power generation capability," *IET Generation, Transmission and Distribution*, vol. 11, no. 15, pp. 3791–3800, 2017, doi: 10.1049/IET-GTD.2016.1246.
- [20] A. Parida and D. Chatterjee, "Model-based loss minimisation scheme for wind solar hybrid generation system using (grid-connected) doubly fed induction generator," *IET Electric Power Applications*, vol. 10, no. 6, pp. 548–559, 2016, doi: 10.1049/iet-epa.2016.0040.
- [21] S. J. Rind, Y. Ren, K. Shi, L. Jiang, and M. Tufail, "Rotor flux-MRAS based speed sensorless non-linear adaptive control of induction motor drive for electric vehicles," *Proceedings of the Universities Power Engineering Conference*, vol. 2015-November, 2015, doi: 10.1109/UPEC.2015.7339869.




- [22] M. Rashed and A. F. Stronach, "A stable back-EMF MRAS-based sensorless low-speed induction motor drive insensitive to stator resistance variation," *IEE Proceedings: Electric Power Applications*, vol. 151, no. 6, pp. 685–693, 2004, doi: 10.1049/ip-epa:20040609.
- [23] A. V. Ravi Teja, V. Verma, and C. Chakraborty, "A New Formulation of Reactive-Power-Based Model Reference Adaptive System for Sensorless Induction Motor Drive," *IEEE Transactions on Industrial Electronics*, vol. 62, no. 11, pp. 6797–6808, 2015, doi: 10.1109/TIE.2015.2432105.
- [24] A. V. Ravi Teja, C. Chakraborty, S. Maiti, and Y. Hori, "A new model reference adaptive controller for four quadrant vector controlled induction motor drives," *IEEE Transactions on Industrial Electronics*, vol. 59, no. 10, pp. 3757–3767, 2012, doi: 10.1109/TIE.2011.2164769.
- [25] M. R. A. Kashkooli and M. G. Jovanović, "Parameter independent control of doubly-fed reluctance wind generators without a rotor position sensor," *International Journal of Electrical Power and Energy Systems*, vol. 137, 2022, doi: 10.1016/j.ijepes.2021.107778.

BIOGRAPHIES OF AUTHORS



Adikanda Parida    received the M.Tech. Degree in industrial systems and drives from RGPV, Bhopal, India, 2005, and a Ph.D. degree in electrical engineering department from Jadavpur University, Kolkata, India. His research interests include hybrid renewable power generation, rural electrification, energy conservation, and management. He is a member of IEEE. He can be contacted at email: adikanda_2003@yahoo.co.in.



Manish Paul    received the Master in Technology in Electrical Engineering from NIT Agartala in 2014 and Bachelor in Technology in Electrical Engineering from NERIST, Arunachal Pradesh in 2010. He is currently a Research Scholar with the Department of Electrical Engineering, NERIST, Arunachal Pradesh, India. His research interests include electric motor drives, wind energy conversion, control of doubly fed machines for variable speed applications, and reluctance machine. He can be contacted at email: manishpaul1988@gmail.com.